Available online at www.sciencedirect.com
ScienceDirect
Journal of Nuclear Materials 360 (2007) 16–24
journal of nuclear materials
www.elsevier.com/locate/jnucmat

Thermal and physical properties of molten fluorides for nuclear applications

J.P.M. van der Meer, R.J.M. Konings *

European Commission, Joint Research Centre, Institute for Transuranium Elements, P.O. Box 2340, 76125 Karlsruhe, Germany

Abstract

$LiF–BeF_2–ThF_4$ is a key system in molten salt reactor fuel studies. In this paper we give an overview of some important features of this ternary system. We discuss the phase behavior, vapor pressure, density and viscosity, based on what is known in the literature and on our own data from previous work on the thermodynamic assessment of $LiF–BeF_2–ThF_4$.

1. Introduction

The Generation IV initiative promotes the development of the future-generation nuclear energy systems, which are economical, safe and clean. One of the selected reactor concepts in this programme is the molten salt reactor (MSR). In a MSR, the fuel is dissolved in a circulating molten fluoride salt mixture. This principle was developed in the 1960s in Oak Ridge National Laboratory, USA. The massive number of studies stemming from this period form a base for the present MSR designs.

The MSR can be designed to breed uranium from thorium in a thermal or epi-thermal neutron spectrum. ^{232}Th captures a neutron, becoming ^{233}Pa. This decays with a half-life of 27 days to ^{233}U, which is a fissile isotope. The matrix, in which the actinides are dissolved, not only needs to offer the best neutronic conditions facilitating this reaction, but also to meet other thermal and physico-chemical requirements, such as the resistance against radiation, the thermal stability and the capacity to dissolve both actinides and fission products. It has appeared that a $^7LiF–BeF_2$ mixture is the most appropriate solvent.

$LiF–BeF_2–ThF_4$ is therefore a key system in the molten salt reactor studies. Numerous studies exist on the binary subsystems, especially on $LiF–BeF_2$, considering several aspects, as phase behavior [1–6], density [7,8] and viscosity [8,9]. However, studies on the characteristics of the ternary systems are scarce. In this work we give an overview on the phase behavior, vapor pressure, density and viscosity of the $LiF–BeF_2–ThF_4$ system.

2. Thermodynamic assessment of $LiF–BeF_2–ThF_4$

We performed the assessment for the ternary and the binary subsystems of $LiF–BeF_2–ThF_4$ in a previous study [10], where the thermodynamic data of the

* Corresponding author. Tel.: +49 7247 951 391; fax: +49 7247 951 99391.
E-mail address: rudy.konings@ec.europa.eu.int (R.J.M. Konings).

0022-3115/$ - see front matter © 2006 Elsevier B.V. All rights reserved.
doi:10.1016/j.jnucmat.2006.08.010

components and intermediate compounds in this systems can be found.

2.1. Calculation of the binary phase diagrams

Gibbs energy functions of all phases of the system, including the excess Gibbs energy coefficients of the liquid phase, are necessary to describe a T–X phase diagram. When they are unknown, they can be obtained by performing a thermodynamic assessment. The missing coefficients in the Gibbs energy as well as in the excess equations are optimized so that a best fit is found between the known Gibbs energy functions of the phases and the available experimental data.

The Gibbs energy functions for the relevant compounds are described by Eq. (1) as the contribution of the enthalpy of formation and the absolute entropy at the reference state plus a contribution of the heat capacity C_p as a polynomial function of T.

$$G(T) = \Delta_f H^0(298.15\ \mathrm{K}) - S^0(298.15\ \mathrm{K})T + T\ln(T) + \sum a_i T^i. \quad (1)$$

All optimizations were done using the OptiSage module in the FactSage 5.4 software package [11]. It was assumed that, according to the Neumann–Kopp rule, the C_p could be added in weighted average of the pure compounds, whereas the enthalpy and entropy of formation needed to be assessed.

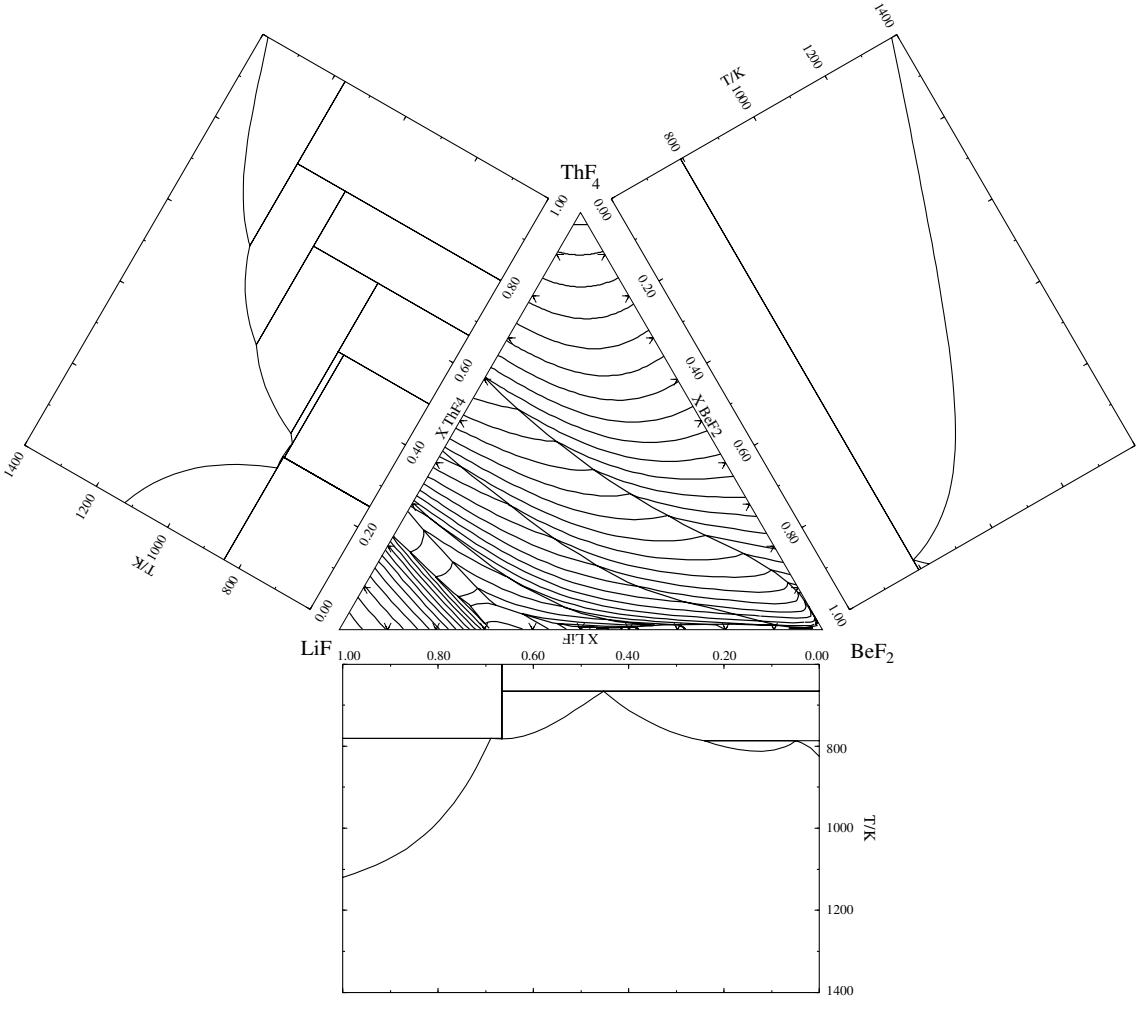

Fig. 1. The projection of the liquidus surface of LiF–BeF_2–ThF_4. Isotherms with an interval of 25 K are shown. The three binary subsystems are along the sides.

Table 1
Calculated invariant equilibria in $LiF–BeF_2–ThF_4$

X_{LiF}	X_{BeF_2}	X_{ThF_4}	T/K	Type invariant	Phases present
0.70	0.24	0.06	758.9	Eutectic[c]	$LiF + 3LiF \cdot ThF_4 + 2LiF \cdot BeF_2 + L$
0.65	0.29	0.06	754.7	Peritectic	$3LiF \cdot ThF_4 + LiF \cdot ThF_4 + 2LiF \cdot BeF_2 + L$[b]
0.48	0.515	0.005	662.9	Eutectic	$2LiF \cdot BeF_2 + BeF_2 + LiF \cdot ThF_4 + L$[b]
0.34	0.65	0.01	751.0	Peritectic	$LiF \cdot ThF_4 + LiF \cdot 2ThF_4 + BeF_2 + L$[b]
0.10	0.89	0.01	783.8	Peritectic	$LiF \cdot 2ThF_4 + LiF \cdot 4ThF_4 + BeF_2 + L$[b]

General polynomials were used to describe the excess Gibbs energy coefficients of the liquid phase that define the shape of the phase diagram. The equation for a binary system A–B is given in Eq. (2).

$$\Delta_{xs}G = \sum_{p,q=0}^{n} L_{A,B}^{p,q}(T) Y_A \left(\frac{\chi_i}{\chi_i + \chi_j}\right)^p Y_B \left(\frac{\chi_j}{\chi_i + \chi_j}\right)^q, \tag{2}$$

$L_{A,B}^{p,q}(T)$ is the excess Gibbs energy term as a function of the temperature. Y_A and Y_B are the equivalent fractions of the components, while χ_i and χ_j are the sum of the equivalent fractions in the same symmetry group with i and j as indices for the group numbers. The optimized excess Gibbs coefficients of $LiF–BeF_2$, $LiF–ThF_4$ and $BeF_2–ThF_4$ can be found in [12].

2.2. Calculation of the ternary diagram

The ternary phase diagram was obtained by extrapolation of the binary interaction coefficients. Several ways exist to do this, taking into account the weight of the components involved. A symmetrical extrapolation, for example the Muggianu method, would be suitable for a system in which the components exert a similar chemical behavior, like NaF–KF–RbF. As $LiF–BeF_2–ThF_4$ is not chemically symmetric, the Kohler–Toop method was applied, which handles the extrapolation for chemically asymmetric systems. LiF was selected as the asymmetric component, since it is highly ionic, whereas BeF_2 and ThF_4 have the tendency to form ions with a molecular character as BeF_4^{2-} [13] and ThF_6^{2-} in the melt.

In Fig. 1 a projection of the liquidus surface of the ternary system is shown, together with the three binary subsystems. The molar compositions and the temperatures of the calculated invariant equilibria are listed in Table 1. The calculated melting temperature of the typical molten salt breeder fuel composition ($0.717LiF–0.16BeF_2–0.12ThF_4–0.003UF_4$ [14], in this case simplified to $0.717LiF–0.16BeF_2–0.123ThF_4$) is 794.5 K. This is slightly higher than the experimental value of 773 ± 5 K, which was reported by Cantor et al. [15].

3. Vapor pressure

Low vapor pressures at the operating temperature are desirable for safety reasons. The partial vapor pressures of the gaseous phase were calculated in the temperature range 400–1500 K for the typical molten salt breeder fuel, as mentioned in Section 2. The calculations were performed using the Equilib module in the FactSage software package. $\Delta_f H^0$ (298.15 K), S^0 (298.15 K) and C_p for the gaseous phase for every component present in the vapor were needed to calculate the partial and the total vapor pressures. The values were extracted from the NIST-JANAF thermochemical tables [16] and are listed in Table 2. For the liquid phase the solution model as presented in Section 2 was used.

Fig. 2 shows the partial and total vapor pressures of the molten salt breeder fuel composition. LiF also exists as a dimer, Li_2F_2, in the gas, and mixed Li_nBeF_{2+n} species also have been taking into account. It can be seen that over the whole temperature range the total vapor pressure is dictated by BeF_2. In the range 750–900 K, in which the MSR will operate, the total pressure increases from 10^{-8} to 10^{-6} bar. This is a low value and it proves that this fluoride mixture meets the demand of a low vapor pressure in a MSR system at working temperatures.

Cantor et al. [15] investigated the vapor pressure of MSBR fuel. He proposed a pressure–temperature relation according to Eq. (3). This function is also plotted in Fig. 2 and it can be seen that the agreement between the calculated and the experimental values is good.

$$^{10}\log(p/\text{Torr}) = 8.0 - \frac{10\,000}{T/\text{K}}. \tag{3}$$

Eq. (3) was estimated from the vapor pressure measurements of $LiF–BeF_2$ mixtures by Cantor et al.

Table 2
$\Delta_f H^0$ (298.15 K), S^0 (298.15 K) and C_p data for the components in the gas phase with composition 0.717LiF–0.16BeF_2–0.123ThF_4

X	$\Delta_f H^0$ (298.15 K)/ kJ mol^{-1}	S^0 (298.15 K)/ J K^{-1} mol^{-1}	a	bT/K	cT^2/K^2	dT^3/K^3	eT^{-2}/K^{-2}
LiF	−340.575	200.28	32.31	7.513×10^{-3}	-3.249×10^{-6}	5.010×10^{-10}	-2.657×10^{5}
Li_2F_2	−942.781	258.63	79.21	3.470×10^{-3}	-7.641×10^{-7}		-1.515×10^{6}
$LiBeF_3$	−1390.30	292.58	113.2	2.995×10^{-3}	2.701×10^{-6}	5.008×10^{-10}	-1.144×10^{4}[b]
Li_2BeF_4	−1958.20	324.45	173.4	-3.112×10^{-3}	-1.001×10^{-6}	3.217×10^{-10}	-1.979×10^{4}[b]
BeF_2	−796.190	227.56	47.30	1.895×10^{-2}	-8.438×10^{-6}	1.259×10^{-9}	-5.216×10^{5}
ThF_4[a]	−1748.2	351.56	122.4	-1.406×10^{-2}	7.365×10^{-6}	-1.939×10^{-9}	-7.545×10^{3}[b]

[a] An extra term appeared to fit the C_p function optimally: $2.011\times10^{-13}T^4$/K^4.
[b] This coefficient is eT^{-1}/K^{-1}.

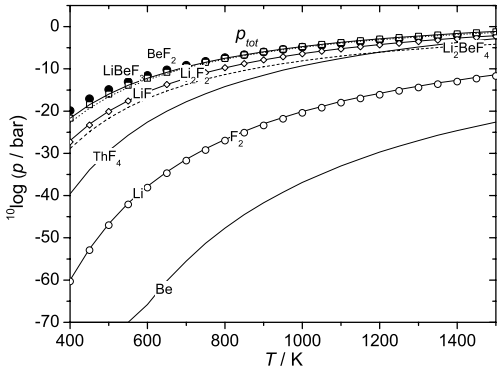

Fig. 2. The partial and total vapor pressures of a typical molten salt breeder fuel composition. Plotted as well is the total vapor pressure (●) as given by Cantor et al. [15].

[17]. Compared were the mixtures with the same LiF/BeF_2 ratio as in MSBR fuel, which is 81.8 mol% LiF to 18.2 mol% BeF_2. At $T = 1273$ K, $^{10}\log(p/\text{bar})$ is −2.48 and at $T = 1373$ K $^{10}\log(p/\text{bar})$ is −1.93. The calculated total vapor pressure $^{10}\log(p_{calc}/\text{bar})$ for LiF–BeF_2 at the same conditions was −2.43, respectively −1.75, which is in good agreement with the experimental values.

4. Density of MSR breeder fuel

4.1. The density of mixtures

Engineers need to know the density of the fuel mixture for the reactor design. Densities of pure components are usually known, but data the densities of mixtures are more scarce. In this section it is investigated how the density of mixtures can be derived from the density of the pure components.

The density ρ is defined as the ratio of the molar weight M and the molar volume V_m

$$\rho/\text{kg m}^{-3} = \frac{M/10^3\ \text{g mol}^{-1}}{V_m/\text{m}^3}. \quad (4)$$

The molar weight of a mixture is simply the sum of the molar weights of its components

$$M = \sum N_i M_i. \quad (5)$$

For the molar volume this is only the case for ideal mixtures:

$$V_{idm} = \sum N_i V_i, \quad (6)$$

resulting in a linear variation as a function of composition in case of a binary system. In practice many mixtures are not ideal but real, and deviations from the linearity can be observed

$$V_m = V_{idm} + V_{exs}. \quad (7)$$

It should be noted that the melting point of a mixture is often much lower than that of the end member compounds, and the measurements for the mixture are made in a temperature range where the liquid phases of the end member compounds are thermodynamically not stable. In that case the experimental molar volume of the end-member compounds is extrapolated to the supercooled state.

4.2. LiF–BeF_2

The density of liquid LiF–BeF_2 has been measured by Blanke et al. [7] from 0 to 55 mol% BeF_2, and Cantor et al. [8] for 50.2, 74.9 and 89.2 mol% BeF_2. The results are shown in Fig. 3 in an isothermal section for $T = 1073$ K of the molar volume. This figure confirms the linear dependence on the mole fraction and thus the additivity of the molar volumes. It can also be seen that the result of Cantor [18] is in perfect agreement with the relation based on the experimental molar volume of BeF_2

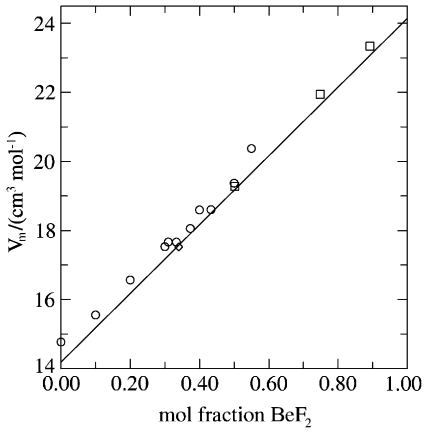

Fig. 3. The molar volume of liquid LiF–BeF_2 at 1073 K; (○) Blanke et al. [7]; (□) Cantor et al. [8]; (◊) Cantor [18]; the line represents V_m of the ideal mixture.

and the extrapolated molar volume of LiF in the supercooled state.

4.3. LiF–ThF_4

The density of LiF–ThF_4 mixtures was measured by Porter and Meaker [19] and Hill et al. [20]. The results are in good agreement and clearly indicate a linear dependence of the molar volume with composition, confirming ideal behavior, which is shown in Fig. 4.

4.4. BeF_2–ThF_4

The density of liquid BeF_2–ThF_4 has not been determined experimentally. However, the density

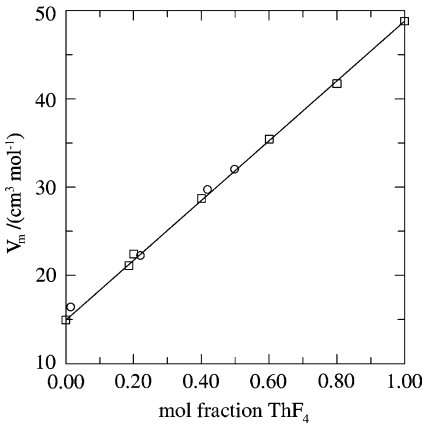

Fig. 4. The molar volume (right) of liquid LiF–ThF_4 at 1273 K; (○) Porter and Meaker [19]; (□) Hill et al. [20]; the line represents V_m of the ideal mixture.

Table 3
The molar volumes of three LiF–BeF_2–ThF_4 mixtures at $T = 1073$ K

Molar composition			V_m/cm^3 mol^{-1}	
X_{LiF}	X_{BeF_2}	X_{ThF_4}	$V_{m,exp}$	$V_{m,cal}$
0.7011	0.2388	0.0601	20.0	20.0
0.7006	0.1796	0.1198	21.4	21.6
0.6998	0.1499	0.1503	22.4	22.4

The experimental values from Cantor [18] and the calculated values from the end-members.

of the liquid of the analogous system BeF_2–UF_4 was measured by Blanke et al. [7], though only for a single composition (35 mol% UF_4). The molar volume derived from this value (30.4 cm^3 mol^{-1} at $T = 1073$ K) is in reasonable agreement with the value calculated for an ideal mixture of the pure components (31.9 cm^3 mol^{-1}), taking into account the uncertainties of the value for BeF_2.

4.5. LiF–BeF_2–ThF_4

Since the molar volumes of the liquid phases of the LiF–BeF_2 and LiF–ThF_4 binaries show ideal behavior, the same can be assumed for the LiF–BeF_2–ThF_4 ternary. The densities in the ternary can thus be simply calculated from the molar volume and the molar weight.

The density of LiF–BeF_2–ThF_4 of three compositions with almost constant LiF concentration was measured by Cantor [18]. As shown in Table 3, the molar volumes derived from these data are in excellent agreement with those calculated from the pure components.

5. Viscosity of LiF–BeF_2–ThF_4

As density, viscosity is also a key parameter for reactor design. Data on the pure components are known, but data on the viscosity of mixtures are more scarce. In this section we investigate ways to estimate the viscosity of a ternary mixture.

The dynamic viscosity of a melt can be related to the Gibbs energy of activation for viscous flow, ΔG^*, by Eq. (8).

$$\eta = \frac{Nh\rho}{M} \exp\left(\frac{\Delta G^*}{RT}\right), \tag{8}$$

where ρ is the density of the melt in kg m^{-3}, h is Planck's constant, N is Avogadro's number, M is molecular weight in kg mol^{-1}, T is the absolute

temperature in K and R is the universal gas constant. Seetharaman et al. [21] proposed a method to estimate the viscosity of ternary silicate melts by suggesting that ΔG^* is the sum of the ideal activation energy for viscous flow and the thermodynamic excess Gibbs energy of mixing. We attempted to follow his method for our ternary fluoride system. However, when applying this method to the fluorides, we did not find a good result using the thermodynamical excess Gibbs energy of mixing.

We suggest that the viscosity of a ternary system can be described in a similar way as the thermodynamic properties of the liquid phase in a ternary diagram. Analogously to the thermodynamic Gibbs energy of mixing in a solution phase, which exists of a sum of the Gibbs energy of the pure components and a mixing term, the viscosity can be described as the sum of the activation energy of the pure components (the ideal part) plus an extra term that covers the mixing part of the activation energy in a multicomponent system, as in Eq. (9).

$$\Delta G^* = \Delta_{id} G^* + \Delta_{ex} G. \tag{9}$$

Data on the viscosity of LiF–BeF_2 [8,9] and LiF–ThF_4 [22], which are plotted in Fig. 5, respectively Fig. 6, were used to derive the excess activation energy terms. For each composition, the viscosity η was given, such that every η is valid for a certain temperature range. By η, defined in Eq. (8), the total ΔG^* is known and its T-dependence can be fitted as a first order polynomial '$a + bT$'. So for every composition and temperature, ΔG^* can be calculated. The weighted average of ΔG^* for the pure components is the ideal term $\sum_i X_i \Delta G_i^*$. The excess Gibbs energy of activation for LiF–BeF_2 and LiF–ThF_4, calculated as the total ΔG^* minus the ideal part,

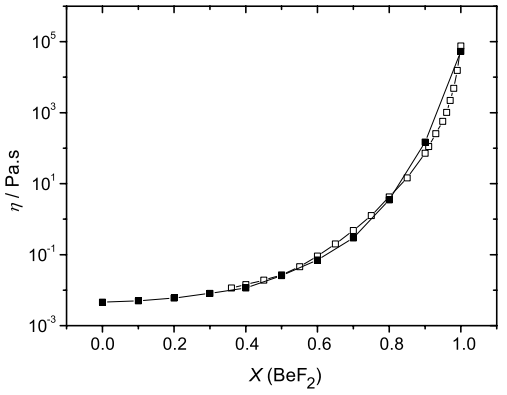

Fig. 5. The dynamic viscosity of LiF–BeF_2 at 873 K by Cantor et al. [8] (□) and Desyatnik et al. [9] (■).

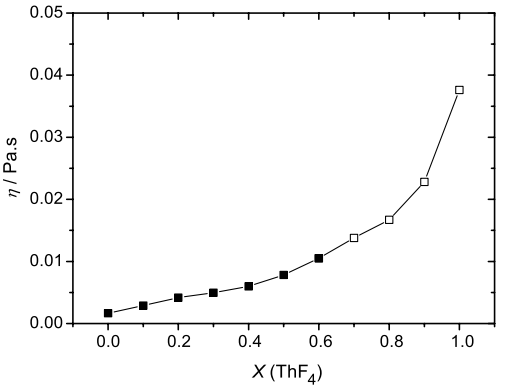

Fig. 6. The dynamic viscosity of LiF–ThF_4 at 1200 K by Chervinskii et al. [22]. Open symbols indicate the extrapolation of the viscosity function in the supercooled region.

can be described as the Redlich-Kister polynomials in Eq. (10), respectively Eq. (11). $\Delta_{ex} G$ is plotted for LiF–BeF_2 and LiF–ThF_4 in Fig. 7.

$$\Delta_{ex} G^*_{LiF-BeF_2} = X_{BeF_2} X_{LiF} (-284015 \cdot X_{BeF_2} - 57618 \cdot X_{LiF}), \tag{10}$$

$$\Delta_{ex} G^*_{LiF-ThF_4} = X_{ThF_4} X_{LiF} (-22110 \cdot X_{ThF_4} + 17081 \cdot X_{LiF}). \tag{11}$$

The viscosity of BeF_2–ThF_4 is not known. However, we treat the system LiF–BeF_2–ThF_4 as a binary system with xLiF–$(1-x)BeF_2$ as one and xLiF$(1-x)ThF_4$ as the other end-member. Basically, the system is reduced as the sum of pseudobinary systems BeF_2–ThF_4 with a constant molar fraction of LiF. Eqs. (10) and (11) are substituted in Eq. (9) to calculate the activation energy for viscous flow. It should be noted that calculating the ternary viscosity by this way was analogous to the calculation of ternary phase diagrams from the binaries, where one would speak of an asymmetrical extrapolation, with LiF as the asymmetric component, exactly as was done for the LiF–BeF_2–ThF_4 diagram. By using Eq. (8), the viscosity of LiF isopleths in LiF–BeF_2–ThF_4 could be calculated. Plotted in Fig. 8 is the viscosity for BeF_2–ThF_4 at a constant molar fraction of LiF = 0.70, since this is approximately the fraction of LiF in MSBR fuel.

A few data are available for the viscosity in LiF–BeF_2–ThF_4. One data point was reported by MacPherson [23] and three by Cantor et al. [15] for $X_{LiF} = 0.70$. It can be seen that the calculated viscosity follows the trend of the experimental data well. Also the values of model and data are in agreement, considering the uncertainty range of 25% for the experimental data indicated by Cantor.

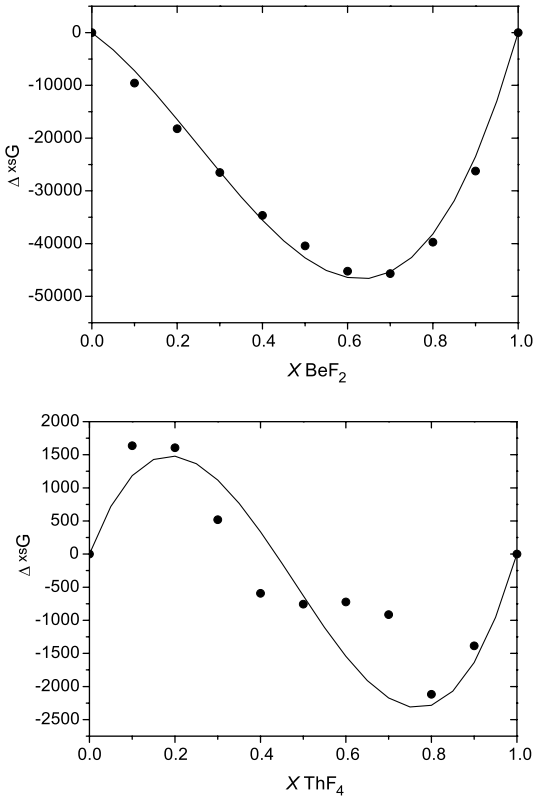

Fig. 7. The excess activation energy for viscous flow for LiF–BeF_2 and LiF–ThF_4, fitted with a Redlich-Kister polynomial.

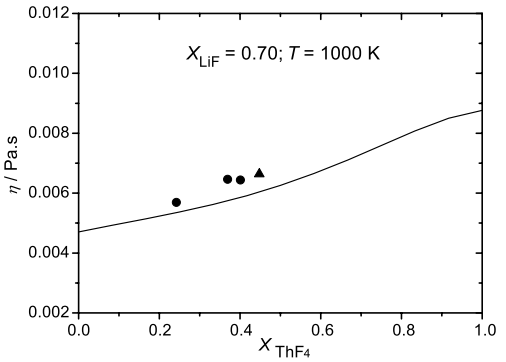

Fig. 8. The pseudobinary ThF_4–BeF_2 viscosity diagram at 1000 K; at a constant molar fraction of LiF = 0.70. (▲) MacPherson [23]; (●) Cantor et al. [15].

However, concise conclusions cannot be drawn from the comparison with four data points. More data are needed to study the viscosity model used here in more detail. To complete the model, we would need viscosity measurements on the binary BeF_2–ThF_4 system and further viscosity data on the ternary system would be desirable as well.

6. Conclusion

The phase behavior, vapor pressure, density and viscosity of the candidate system for molten salt breeder fuel, LiF–BeF_2–ThF_4 have been calculated. A typical composition is 0.717LiF–0.16BeF_2–0.12ThF_4–0.003UF_4, which is in this case simplified to 0.717LiF–0.16BeF_2–0.123ThF_4. The temperature of fusion, according to our calculated phase diagram, is 794.5 K, which is in agreement, but slightly higher than the 773 ± 5 K, reported by Cantor et al. [15].

The vapor pressure of this composition at the operating temperature of a MSR (750–900 K) is low, namely between 10^{-8} and 10^{-6} bar. It is fully dictated by the partial vapor pressure of BeF_2.

A linear relationship exists between the density of the pure molten fluoride components and the density of a liquid mixture. The density of MSR fuel could therefore be calculated as the weighted average from the densities of liquid LiF, BeF_2 and ThF_4. The calculated and the experimental values were in perfect agreement: 21.6, respectively 21.4 $cm^3\ mol^{-1}$.

The dynamic viscosity of a molten fluoride mixture can be calculated from the activation energy for viscous flow. This consists, analogously to the thermodynamic Gibbs energy of mixing, of an ideal and an excess part. The excess activation energy was derived from the viscosity data on LiF–BeF_2 and LiF–ThF_4 and was described as Redlich-Kister polynomials. The viscosity of LiF–BeF_2–ThF_4 at a constant molar fraction of LiF = 0.70 was calculated and compared to the few data available. It appeared that the values obtained from the model about 6.0×10^{-3} Pa s, were in agreement with the measured values by ORNL researchers. However, the number of data are too scarce to draw conclusions. More data on binary and ternary systems are needed for a better understanding of viscous flow in molten fluorides.

Appendix A. Density and viscosity of the pure compounds

A.1. LiF

The density of LiF in the liquid phase has been measured by Kostyukov and Polyakova (cited in [24]), Porter and Meaker [25], Hill et al. [20], Smirnov et al. [26], Hara and Ogino [27], and Chekhovskoi [28]. The results of Hill et al. [20], Smirnov et al. [26], Hara and Ogino [27] are in good agreement, as

shown in Fig. 9. The recommended equation, based on these results, is

$$\rho/(\mathrm{kg\,m^{-3}}) = 2320.7 - 0.459(T/\mathrm{K}). \quad (A.1)$$

The viscosity of liquid LiF has been measured by several authors (Fig. 10): Vetyukov and Sipriya [24], Smirnov et al. [26], Desyatnik et al. [9], and Abe et al. [29]. The results are in reasonable agreement, as shown in Fig. 10. We consider the results of Abe et al. [29] and Desyatnik et al. [9], which are almost identical, to be the most reliable as they are made on well-defined samples and with well qualified equipment. We recommend the equation by Abe et al. [29], which covers a much wider temperature range

$$\eta/(\mathrm{mPa\,s}) = 0.11494\exp(3246.8/(T/\mathrm{K})). \quad (A.2)$$

A.2. BeF_2

The density of liquid BeF_2 was measured by MacKenzie [30] using the Archimedean method to be $(1947 \pm 10)\ \mathrm{kg\,m^{-3}}$ at 1073 K. Cantor et al. [8] also measured the density by the Archimedean method, but due to experimental difficulties derived only an approximate value, $1960\ \mathrm{kg\,m^{-3}}$ at 1123 K. The value of MacKenzie is recommended.

The viscosity of liquid BeF_2 was measured by Mackenzie [30] from 973 to 1223 K, Moynihan and Cantor [31] from 847 to 1252 K and Desyatnik et al. [9] from 1104 to 1333 K, as part of their systematic studies of the viscosity of LiF–BeF_2 mixtures. The results of these studies are in excellent agreement, see Fig. 11. We recommend the equation by Moynihan and Cantor [31], which is a polynomial equation

$$\log(\eta/\mathrm{mPa\,s}) = -8.119 + 1.1494\times10^{4}(T/\mathrm{K})^{-1} + 6.39\times10^{5}(T/\mathrm{K})^{-2}. \quad (A.3)$$

A.3. ThF_4

The density of liquid ThF_4 has been measured by Kirshenbaum and Cahill [32] from 1393 to 1651 K and Hill et al. [17,20] from 1392 to 1508 K. The results differ considerably as is shown in Fig. 12. Desyatnik et al. [33] measured the densities of NaF–ThF_4 and KF–ThF_4 systems up to 80 mol% ThF_4. Extrapolation of these results to 100 mol% ThF_4 gives values close to the results of Kirshenbaum and Cahill [32]. For that reason the recommended equation is this solely based on these results

$$\rho/(\mathrm{kg\,m^{-3}}) = 7108 - 0.759(T/\mathrm{K}). \quad (A.4)$$

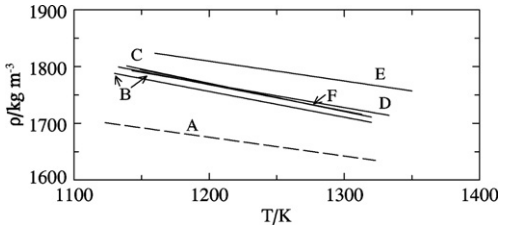

Fig. 9. The density of liquid LiF: curve (A) Porter and Meaker [25]; (B) Hara and Ogino [27]; (C) Hill et al. [20]; (D) Smirnov et al. [26]; (E) Chekhovskoi. [28]; (F) Yaffe and Van Artsdalen [34].

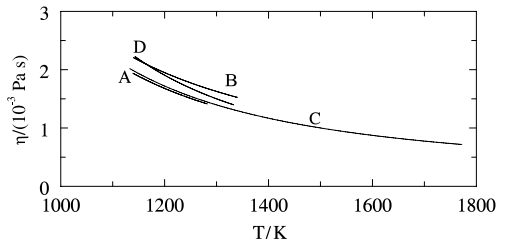

Fig. 10. The viscosity of liquid LiF: curve (A), Desyatnik et al. [9]; (B) Sipriya and Vetyukov [24]; (C) Abe et al. [29]; (D) Smirnov et al. [26].

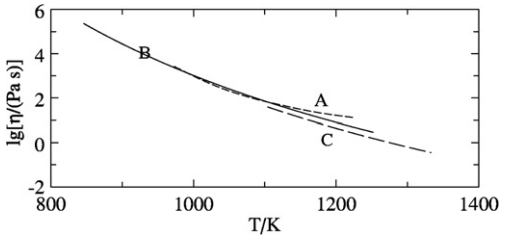

Fig. 11. The viscosity of liquid BeF_2: curve (A) Mackenzie [30]; (B) Moynihan and Cantor [31]; (C) Desyatnik et al. [9].

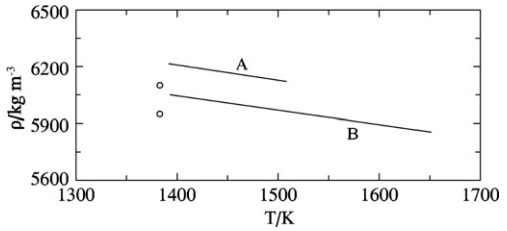

Fig. 12. The density of liquid ThF_4: curve (A) Hill et al. [17,20]; (B) Kirshenbaum and Cahill [32]; the circles show the values extrapolated from the measurements of the NaF–ThF_4 and KF–ThF_4 systems by Desyatnik et al. [33].

The viscosity of pure liquid ThF_4 was measured by Desyatnik et al. [33] from 1393 to 1481 K. The results are represented by the equation:

$$\eta/(\text{mPa s}) = 0.0279\exp(8563/(T/\text{K})). \quad \text{(A.5)}$$

References

[1] E. Thilo, H.-A. Lehmann, Z. Anorg. Chem. 258 (1949) 332.
[2] D.M. Roy, R. Roy, E.F. Osborn, J. Am. Ceram. Soc. 33 (1950) 85.
[3] D.M. Roy, R. Roy, E.F. Osborn, J. Am. Ceram. Soc. 37 (1954) 300.
[4] A.V. Novoselova, Y.P. Simanov, E.I. Jarembash, Zh. Fiz. Khim. SSSR 26 (1952) 1244.
[5] R.E. Thoma, H. Insley, H.A. Friedman, G.M. Hebert, J. Nucl. Mater. 27 (1968) 166.
[6] K.A. Romberger, J. Braunstein, R.E. Thoma, J. Phys. Chem. 76 (1972) 1154.
[7] B.C. Blanke, E.N. Bousquet, M.L. Curtis, E.L. Murphy, Tech. Rep. USAEC MLM-1086 (1956).
[8] S. Cantor, W.T. Ward, C.T. Moynihan, J. Chem. Phys. 50 (1969) 2874.
[9] V.N. Desyatnik, A.I. Nechaev, Y.F. Chervinskii, Zh. Prik. Kh. 54 (1981) 2310.
[10] J.P.M. van der Meer, R.J.M. Konings, M.H.G. Jacobs, H.A.J. Oonk, J. Nucl. Mater. 344 (2005) 94.
[11] C.W. Bale, P. Chartrand, S.A. Degterov, G. Eriksson, K. Hack, R. BenMahfoud, J. Melançon, A.D. Pelton, S. Petersen, CALPHAD 62 (2002) 189.
[12] J.P.M. van der Meer, R.J.M. Konings, H.A.J. Oonk, J. Nucl. Mater., in press.
[13] F. Vaslov, A.H. Narten, J. Chem. Phys. 59 (1973) 4949.
[14] W.R. Grimes, Nucl. Appl. Tech. 8 (1970) 137.
[15] S. Cantor, J.W. Cooke, A.S. Dworkin, G.D. Robbins, R. E. Thoma, G.M. Watson, Tech. Rep. Report ORNL-TM-2316, August (1968).
[16] M.W. Chase Jr. (Ed.), NIST-JANAF Thermochemical Tables, fourth ed., J. Phys. Chem. Ref. Data Monograph 9.
[17] S. Cantor, D.S. Hsu, W.T. Ward, Tech. Rep. Report ORNL-3913, March (1966).
[18] S. Cantor, Tech. Rep. ORNL-TM-4308 (1971).
[19] B. Porter, R.E. Meaker, Tech. Rep. BMI RI-6836 (1966).
[20] D.G. Hill, S. Cantor, W.T. Ward, J. Inorg. Nucl. Chem. 29 (1967) 241.
[21] S. Seetharaman, D. Sichen, F.-Z. Ji, Metall. Trans. 31B (2000) 105.
[22] Y.F. Chervinskii, V.N. Desyatnik, A.I. Nechaev, Russ. J. Phys. Chem. 56 (1982) 118.
[23] H.G. MacPherson, Tech. Rep. Report ORNL-2890, October (1959).
[24] M.M. Vetyukov, G.I. Sipriya, J. Appl. Chem (USSR) 46 (1963) 1849.
[25] B. Porter, R.E. Meaker, Tech. Rep. BMI RI-7528 (1971).
[26] M.V. Smirnov, V.P. Stepanov, V.A. Kholkov, Y.A. Shumov, A.A. Antonov, Russ. J. Phys. Chem. 48 (1974) 467.
[27] S. Hara, K. Ogino, ISIJ Int. 29 (1989) 477.
[28] V.Y. Chekhovskoi, Instr. Exp. Tech. 43 (2000) 415.
[29] Y. Abe, O. Kosugiyama, A. Nagashima, J. Nucl. Mater. 99 (1981) 173.
[30] J.D. Mackenzie, J. Chem. Phys. 32 (1960) 1150.
[31] C.T. Moynihan, S. Cantor, J. Chem. Phys. 48 (1968) 115.
[32] A.D. Kirshenbaum, J.A. Cahill, J. Inorg. Nucl. Chem. 19 (1961) 65.
[33] V.N. Desyatnik, A.A. Klimenkov, N.N. Kurbatov, A.I. Nechaev, S.P. Raspopin, Y.F. Chervinskii, Sov. Atom. Energy 51 (1981) 807.
[34] I.S. Yaffe, E.R. van Artsdalen, Tech. Rep. ORNL-2159 (1956).